

# Submillimeter spectroscopy for chemical analysis with absolute specificity

Ivan R. Medvedev,<sup>1</sup> Christopher F. Neese,<sup>1</sup> Grant M. Plummer,<sup>2</sup> and Frank C. De Lucia<sup>1,\*</sup>

<sup>1</sup>Department of Physics, Ohio State University, 191 W. Woodruff Avenue, Columbus, Ohio 43210, USA

<sup>2</sup>Enthalpy Analytical, Inc., 2202 Ellis Road, Durham, North Carolina 27703, USA

\*Corresponding author: fcd@mps.ohio-state.edu

Received December 21, 2009; revised March 9, 2010; accepted March 19, 2010;  
posted April 2, 2010 (Doc. ID 121787); published May 5, 2010

A sensor based on rotational signatures in the submillimeter (SMM) region is described. This sensor uses frequency synthesis techniques in the region around 10 GHz, with nonlinear diode frequency multiplication to 210–270 GHz. This provides not only a nearly ideal instrument function, but also frequency control and agility that significantly enhance the performance of the spectrometer as a sensor. The SMM frequencies provide significantly stronger absorptions and broader spectroscopic coverage than lower-frequency microwave systems. Among the characteristics of the sensor are absolute specificity, low atmospheric clutter, good sensitivity, and near-term paths to systems that are both compact and very inexpensive. © 2010 Optical Society of America

OCIS codes: 280.1545, 300.1030, 300.6320, 300.6370, 300.6390, 300.6495.

A resurgence of interest in spectroscopic sensors has been fueled by increases in performance made possible by advances in laser systems and applications in medicine, environmental monitoring, and national security [1–8]. Most of these new approaches make use of the optical–infrared (Op–IR) spectral regions [9–12]. The submillimeter (SMM) spectral region, while much less well known, has also seen significant technological advances [13]. It is possible to use frequency agile, synthesized electronic sources that can be multiplied into the SMM, with power outputs on the order of 1 mW, a power capable of saturating the probed molecules and that corresponds to  $10^{14}$  K in a 1 MHz Doppler linewidth. In the SMM the thermal excitation of many rotational energy levels provides a fingerprint that is complexly redundant *and* resolvable, for even moderately large molecules, because of the small Doppler limit. These fingerprints, contained in more than  $10^5$  resolvable spectral channels, lead to absolute specificity, even in complex mixtures [14,15].

In this Letter we demonstrate new SMM sensors that are comparable with their optical counterparts [1,2,4,7,8] in terms of fractional concentration (ppx, where  $x$  is millions for  $10^6$ , billions for  $10^9$ , trillions for  $10^{12}$ , etc.) sensitivity and are orders of magnitude more favorable than time domain terahertz (TDS-THz) sensors [16,17]. If the sensitivity figure of merit is the amount of sample, the lower optimum pressure ( $\sim 10$  mTorr) of SMM sensors increases their sensitivity by 2–3 orders of magnitude relative to Op–IR sensors. These SMM sensors provide far greater specificity than either, with good speed.

To illustrate the rotational fingerprint, Fig. 1 shows a Doppler-limited rotational spectrum recorded with a backward-wave-oscillator-based fast scan submillimeter spectroscopy technique (FASSST) system [14]. The spectral segment in the bottom panel uses only a small fraction of the available spectral information, shows unambiguous identification

of eight of the species in the mixture<sup>1</sup>, and required only about 10 ms to acquire.

The more compact solid-state sensor system shown in Fig. 2 probes a low-pressure (1–10 mTorr), Doppler-limited sample in the 210–270 GHz region. To provide the required frequency, a  $24\times$  frequency multiplication scheme was adopted. Drive for this system was provided by a fast sweeping 0–400 MHz synthesizer, scanning around a nominal 100 MHz center frequency, which is subsequently mixed with a stepping synthesizer in the 8.75–11.25 GHz range to provide a tunable source offset from the receiver's local oscillator by its intermediate frequency. A YIG (yttrium iron garnet—a kind of microwave filter based on a magnetically tunable resonance) filter was used to select the desired sideband and suppress the many intermodulation products that grow rapidly with frequency multiplication. This frequency control system provides more uniform line shapes and intensities than previous free-running systems [14,18]. We will see below that the frequency stability and agility provided by this approach are very important for the

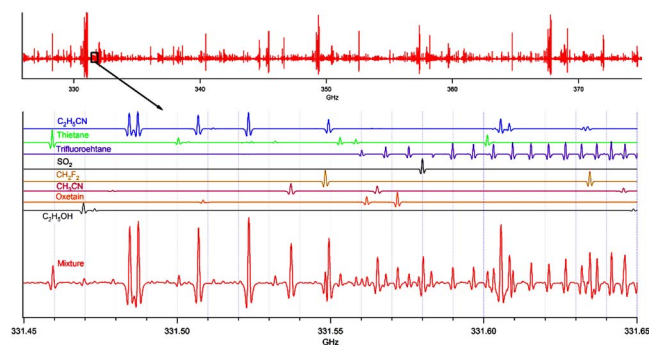


Fig. 1. (Color online) 50 GHz of a spectrum of a mixture of 20 gases on a highly compressed scale taken with a FASSST backward-wave-oscillator-based system (top). 0.4% of this spectrum is expanded to show individual lines (bottom). Comparison with the library spectra of eight gases shows their presence in the gas mixture (middle).

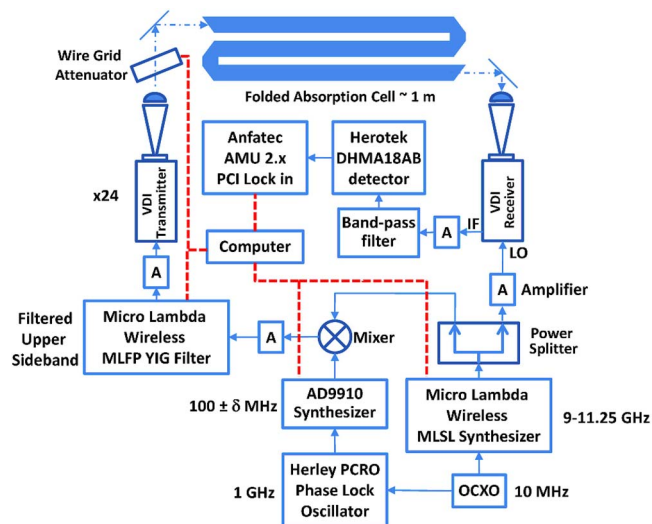


Fig. 2. (Color online) Overview of a SMM frequency multiplication, heterodyne receiver gas sensor. In this system a frequency synthesizer near 10 GHz drives a  $24\times$  diode-based frequency multiplier to provide the local oscillator of a heterodyne receiver. A sideband generation scheme provides synchronized, but offset in frequency, drive to a similar multiplier chain for probe power to the folded 1.2 m absorption cell.

speed, sensitivity, specificity, and clutter rejection of the SMM sensor.

Because molecular saturation often limits probe powers, we chose a heterodyne detector that makes possible a system that approaches fundamental noise limits for low-power probes. Since saturation is determined both by the square of the molecular dipole moment and the pressure, optimal power levels for each molecule and operating condition vary widely. In general we chose a low probe power, a few microwatts, to ensure that under all circumstances we are in a non-saturation limit. For species with smaller dipole moments, it is possible to increase the probe power to increase sensitivity. The local oscillator for this receiver is driven directly by the stepping synthesizer through a similar  $24\times$  multiplier chain. The resulting intermediate frequency signal sweeps around 2.4 GHz ( $100\pm\delta$  MHz  $24\times$ ) and is demodulated by a Schottky diode. An FM modulation, somewhat smaller than the Doppler linewidth, with lock-in detection was used to suppress baseline due to standing waves and other power variations. These power variations can be 5–10 over the 210–270 GHz band. To obtain the desired 1% absolute amplitude calibration, measurements of the DC levels produced by the Schottky diode were used. Library lines of known absorptions allowed us to establish the modulation efficiency. Both the source and the detector operate in the fundamental waveguide, and the power is propagated quasi optically with horns and lenses through a 2.5 cm diameter, 1.2 m long, stainless steel folded cell. Because only a static sample of 1–10 mTorr is required, vacuum is provided by a small turbo and diaphragm pump combination.

The great strength of SMM rotational spectroscopy is its specificity, especially when applied to complex mixtures. Accordingly, we recorded a spectrum at

1 mTorr for each of 32 gases and made mixtures from the gases in this library. This number is considerably larger than is typically used in demonstrations of spectroscopic sensors. While the chosen molecules are generally favorable species for rotational spectroscopy, they range over about 2 orders of magnitude in both strength and spectral density and contain 17 gases included in a common list of toxic industrial chemicals [19]. Many of these species do not have resolved rotational spectra in the Op-IR, and most are considerably less favorable than species typically chosen for demonstrations. Additionally, the near transparency at low pressure in the SMM of  $\text{H}_2\text{O}$  and  $\text{CO}_2$  (molecules that provide significant clutter in Op-IR sensors [4]) makes this approach remarkably clutter free. Whereas  $\text{H}_2\text{O}$  and  $\text{CO}_2$  have atmospheric concentrations of  $\sim 10000$  and 332 ppm, respectively, the first molecule in order of abundance that has even a 1% spectral density at Doppler resolution in the SMM is nitric acid, with an atmospheric concentration in the range of 0.0002–0.05 ppm [20].

Because the information content in the 210–270 GHz region far exceeds that necessary for absolute specificity, we chose a subset of six lines for each gas and observed a 2–6 MHz snippet for each line—a total of 192 snippets and  $\sim 0.5$  GHz of spectral space. These results are shown in Fig. 3. The snippets are recorded in order of the analyte in the library, to facilitate visual identification of detected gases. Automated analyses, based on least-squares (LSQ) techniques and shown in the right-hand panel of Fig. 3, provide quantitative results by comparison of the spectra shown in Fig. 3 with previously recorded libraries. These LSQ analyses require less than 1 s of computation time. Each of the 14 gases placed in the mixture is identified in red in Fig. 3. Those identified in blue are marginal detections that result either from contamination or chemical reactions among the analytes.

Insert a of Fig. 3 shows an enlargement of the ClCN fingerprint region. No ClCN is present in this mixture, and the signal in this region is from the interloping spectra of other species,  $\text{CH}_3\text{CN}$ ,  $\text{C}_2\text{H}_3\text{CN}$ ,  $\text{C}_2\text{H}_5\text{CN}$ , and  $\text{C}_2\text{H}_3\text{F}$ . However, because of the intensity calibration of the system, the fit for the concen-

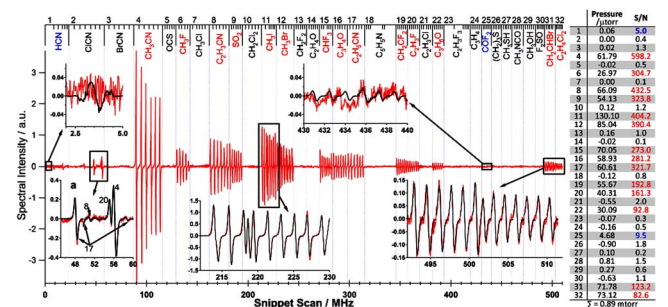


Fig. 3. (Color online) Observed scan spectra at each of the six fingerprint regions selected for each gas for the family of 32 gases considered, with enlargements of specific fingerprint regions. Right, results of a quantitative LSQ analysis. A digital lock-in recovers a near first derivative line shape that results from a small FM modulation in the probe driver.

tration of these four species fully accounts for these spectral features. Accordingly, the fit properly concludes that although there is spectral intensity in the ClCN fingerprint, less than  $0.01 \mu\text{Torr}$  of ClCN is present. The partial pressures of each gas recovered by the LSQ fit ranged from 0.02 to 0.13 mTorr. The total pressure measured spectroscopically was 0.89 mTorr. This pressure is within the accuracy of the pressure measurement of the fill of the sample cell, nominally 1 mTorr.

Because the pressure is low, all of the lines have widths determined by Doppler broadening. Thus the species are spectroscopically noninteracting, and it is possible to determine their minimum detectable concentration individually. If we first consider the strongest species in this figure,  $\text{CH}_3\text{CN}$ , a sample pressure of  $6 \times 10^{-5}$  Torr produces a signal-to-noise ratio S/N of  $\sim 500$  with 0.01 s per point of integration time. Each of the 6 lines has  $\sim 10$  points. If each point receives 1 s of integration time and a fit is used to process all of the information in the  $\sim 60$  points on the lines, the S/N for this recovery becomes  $\sim 40,000$ . Thus, for a 1/1 S/N in the recovery a pressure of  $\sim 1.5 \times 10^{-9}$  Torr would be required. To obtain a ppb measure, the fact that an air pressure of  $\sim 0.1$  Torr can be added without significantly broadening or decreasing the line provides a detectivity level of 15 ppb. Figure 3 also shows that the weakest of the 32 gases ( $\text{C}_2\text{H}_4\text{Cl}_2$ ) is about 30 times weaker, resulting in a detection level of  $\sim 500$  ppb. The most favorable gas, HCN, is about 5 times stronger, resulting in a detection level of  $\sim 3$  ppb. Similar results have been obtained more directly on samples diluted in air.

A comparison of the results presented here with those obtained in a wide variety of Op-IR experiments show that they are similar in terms of ppb sensitivity, with wide variation according to choice of molecule and the trades of technical implementations [1,2,4,7,8]. Because the optimum pressure (which is proportional to the Doppler width and thus to frequency as well) is 100–1000 times smaller in the SMM, in terms of the minimum sample required, the SMM is correspondingly more favorable according to this measure:  $\sim 10^{-14}$  moles for HCN,  $\sim 5 \times 10^{-14}$  moles for  $\text{CH}_3\text{CN}$ , and  $10^{-12}$  moles for  $\text{C}_2\text{H}_4\text{Cl}_2$ . For radicals, for which a strong electronic transition is available, detection limits in the ppt range have been reported [21].

Finally, there is a clear path to even simpler and cheaper systems in the near to medium term. Inexpensive technology is commercially available up to 100 GHz courtesy of the wireless communications industry, and this upper frequency limit is increasing rapidly. While we used instrumentation synthesizers, etc., implementations based on chip level integra-

tions of these functions are available. Finally, the never-ending increase in computational power will further improve our ability to optimize the use of the information content of high-resolution rotational spectra. This combination of analysis power and practicality will allow SMM rotational spectroscopy to take its place alongside other methods as a general analytical and sensor tool in the near term.

We thank the Army Research Office and the Defense Advanced Projects Research Agency (DARPA) for their support of this work.

## References

1. Y. He and B. J. Orr, *Appl. Phys. B* **85**, 355 (2006).
2. M. J. Thorpe, K. D. Moll, R. J. Jones, B. Safdi, and J. Ye, *Science* **311**, 1595 (2006).
3. S. A. Diddams, L. Hollberg, and V. Mbele, *Nature* **445**, 627 (2007).
4. M. J. Thorpe, D. Balslev-Clausen, M. S. Kirchner, and J. Ye, *Opt. Express* **16**, 2387 (2008).
5. T. Gherman and D. Romanini, *Opt. Express* **10**, 1033 (2002).
6. A. A. Kosterev, A. L. Malinovsky, F. K. Tittle, C. Gmachle, F. Capasso, D. L. Sivco, J. N. Baollargeon, A. L. Hutchinson, and A. Y. Cho, *Appl. Opt.* **40**, 5522 (2001).
7. M. Kassi, M. Chenevier, L. Gianfrani, A. Salhi, Y. Rouillard, A. Ouvrard, and D. Romanini, *Opt. Express* **14**, 11142 (2006).
8. I. Vertrillard-Courtillot, T. Gonthiez, C. Clerici, and D. Romanini, *J. Biomed. Opt.* **14**, 064026 (2009).
9. F. Keilmann, C. Gohle, and R. Holzwarth, *Opt. Lett.* **29**, 1542 (2004).
10. S. T. Sanders, *Opt. Photonics News* **16**, 36 (2005).
11. J. Ye, L.-S. Ma, and J. L. Hall, *Opt. Lett.* **21**, 1000 (1996).
12. I. Debecker, A. K. Mohamed, and D. Romanini, *Opt. Express* **13**, 2906 (2005).
13. T. W. Crowe, W. L. Bishop, D. W. Porterfield, J. L. Hesler, and R. M. Weikle, *IEEE J. Solid-State Circuits* **40**, 2104 (2005).
14. S. Albert, D. T. Petkie, R. P. A. Bettens, S. P. Belov, and F. C. De Lucia, *Anal. Chem.* **70**, 719A (1998).
15. I. R. Medvedev, M. Behnke, and F. C. De Lucia, *Appl. Phys. Lett.* **86**, 1 (2005).
16. S. A. Harmon and R. A. Cheville, *Appl. Phys. Lett.* **21**, 2128 (2004).
17. B. Ferguson and X.-C. Zhang, *Nature Mater.* **1**, 26 (2002).
18. I. Medvedev, M. Behnke, and F. C. De Lucia, *Analyst (Cambridge, U.K.)* **131**, 1299 (2006).
19. "Clean Air Act Amendments of 1990," 5.6130, 101st Congress of the United States of America (April 3, 1990).
20. J. H. Seinfeld, *Atmospheric Chemistry and Physics of Air Pollution* (Wiley, 1986).
21. G. Mejean, S. Kassi, and D. Romanini, *Opt. Lett.* **33**, 1231 (2008).